Acc# 735167
DP-MS-80-2

A SMALL-SCALE DEMONSTRATION OF HIGH-LEVEL RADIOACTIVE WASTE PROCESSING AND SOLIDIFICATION USING ACTUAL SRP WASTE

By

J. K. Okeson, R. M. Galloway, E. L. Wilhite,
G. B. Woolsey and R. B. Ferguson

Savannah River Laboratory
E. I. du Pont de Nemours and Company
Aiken, South Carolina 29808

To be presented at the AIChE 89th National Meeting
Portland, Oregon
August 17-20, 1980

This paper was prepared in connection with work under Contract No. DE-AC09-76SR00001 with the U.S. Department of Energy.

DP-MS-80-2

A SMALL-SCALE DEMONSTRATION OF HIGH-LEVEL RADIOACTIVE WASTE PROCESSING AND SOLIDIFICATION USING ACTUAL SRP WASTE

by

J. K. Okeson, R. M. Galloway, E. L. Wilhite,
G. B. Woolsey and R. B. Ferguson

Savannah River Laboratory
E. I. du Pont de Nemours and Company
Aiken, South Carolina 29808

ABSTRACT

A small-scale demonstration of the high-level radioactive waste solidification process by vitrification in borosilicate glass is being conducted using 5-6 liter batches of actual waste. Equipment performance and processing characteristics of the various unit operations in the process are reported and, where appropriate, are compared to large-scale results obtained with synthetic waste.

INTRODUCTION

The Savannah River Plant (SRP) produces nuclear materials for national defense programs and civilian use. These materials are produced by irradiation in nuclear reactors and are recovered by chemical separations processes. The plant is operated by Du Pont for the U.S. Department of Energy. In 26 years of SRP operations, some 63 million gallons of high level radioactive wastes have been generated as a byproduct of the nuclear materials production processes, Figure 1, and new waste is continuing to be generated at a rate of about 1.5 million gallons per year. This waste has been evaporated to 23 million gallons and is now stored in 33 underground carbon steel tanks.

A research and development program has been underway at Savannah River since 1973 to develop and demonstrate appropriate technology for immobilizing this high-level waste in forms suitable for permanent disposal. This paper reports initial results from one of these programs - a small-scale demonstration of the reference SRP solidification process using actual high-level radioactive waste.

Description of SRP Waste and the Reference Waste Immobilization Process

Most wastes from the SRP radiochemical separations processes are initially acidic solutions of heavy metal nitrates. However, before transfer to the carbon steel storage tanks, these solutions are neutralized with sodium hydroxide. This causes precipitation of insoluble oxides and hydroxides of elements present in the fuel or added in reprocessing (primarily Fe, Al, Mn, and Hg) along with most of the fission products and small amounts of actinides and uranium not recovered in reprocessing. After these insoluble materials, referred to as sludge, have settled to the bottom of the waste tank, the supernatant liquid is removed and concentrated by evaporation. The concentrate from the evaporator is transferred to tanks where, on cooling, soluble salts crystallize out. Residual supernate is recycled to the evaporators until these tanks contain only a wet salt cake. The salt cake consists primarily of sodium nitrate and nitrite. Table I gives an average composition for the insoluble solids in SRP sludge and of the soluble salts in the SRP salt cake. A large quantity of supernate also remains in the gelatinous sludge layer as interstitial liquid. The principal radionuclides of biological concern are strontium-90 and plutonium-239, which are found almost exclusively in the sludge, and cesium-137 present in the salt cake and supernate solution.

Figure 2 shows a simplified flowsheet for the reference SRP waste immobilization process. In this process, the salt cake in waste tanks will be redissolved in fresh water while the sludge will be removed from the tanks by hydraulic slurrying techniques.

These two feed streams will then be fed separately into a large shielded building, referred to as the Defense Waste Processing Facility (DWPF), for the remote processing to incorporate the wastes into borosilicate glass.

In the DWPF, the sludge slurry is centrifuged and the cake is washed with fresh water to remove the residual soluble salts entrained in the sludge. The spent wash solution is concentrated by evaporation and combined with the solution formed by dissolving the wet salt cake. The resulting solution is then decontaminated by ion exchange. The ion exchange process removes the cesium from the dissolved salt solution as well as trace amounts of soluble strontium. The decontaminated salt solution is then evaporated and disposed of as low-level waste. The cesium and strontium eluted from the ion exchange columns are mixed with the washed sludge, forming a slurry for feed to the drying and vitrification steps. The slurry is spray-dried in a heated wall dryer and the resulting powder, along with glass frit, falls by gravity into a joule-heated ceramic glass melter. Borosilicate waste glass is poured from the melter into stainless steel canisters which are cleaned and welded shut in preparation for final disposal in a suitable geologic repository. By decontaminating the salt cake and incorporating only the sludge and the cesium and strontium from the salt cake into the borosilicate glass, the total volume of waste glass which must be melted and disposed of is significantly reduced, Figure 3.

Much of the work to develop and demonstrate the SRP reference waste solidification process has been conducted with synthetic nonradioactive waste rather than actual waste. This substitution is essential in order to reduce the cost and difficulty of carrying out the development work. However, a small-scale demonstration of the process is being performed with actual waste retrieved from SRP waste tanks for the purpose of:

- Providing a comparison of synthetic and actual waste processing behavior and product quality.
- Confirming the detailed chemistry of the flowsheet.
- Obtaining basic data on behavior of minor constituents in the ion exchange and vitrification off-gas treatment steps.

The following sections of this paper discuss the results obtained in processing actual waste with small-scale equipment in shielded hot cells.

Sludge Washing

The soluble salts entrained within the sludge at the time it settles to the bottom of the waste tanks must be removed before a high durability borosilicate waste glass can be produced. The sodium sulfate present in the salts is nearly insoluble in borosilicate glass and would form a separate cesium-rich sulfate phase susceptible to rapid leaching if not washed from the sludge before vitrification.

The washing operation consists simply of contacting the sludge with fresh water and then centrifuging the resulting slurry to separate the two phases. Figure 4 shows the experimentally determined amount of soluble salt remaining in both actual and synthetic sludges as a function of the number of washing stages. The lines in Figure 4 are theoretical washing curves calculated from simple dilution principles by the expression:

$$Sn = \frac{Sf}{\left(\frac{W + RI}{RI}\right)^n}$$

where

Sn = mass of soluble salts in washed sludge after n washings

Sf = mass of soluble salts in unwashed sludge feed

W = mass of wash water added in each washing

I = mass of insoluble solids in sludge

R = weight ratio of water retained in sludge to insoluble solids in sludge

For the particular experiments plotted in Figure 4, larger amounts of water, W, were added in each washing stage with the actual sludge than with the synthetic sludge. This is why the salt content of the actual sludge is lower. However, the washing behavior of both actual and synthetic SRP sludges are well described by the dilution washing model. In addition, the ratio, R, of interstitial water to solids in both actual and synthetic sludge has been found to be approximately the same. Thus, the amount of wash water and number of washes required to remove a given amount of salt are nearly the same for both actual and synthetic sludge.

A second important characteristic of the sludge in the washing operation is the ease with which it can be separated from the spent wash water by centrifuging. In tests with actual sludge, a 12-inch diameter imperforate bowl basket centrifuge generating a settling force of 1300 G was used with slurry flow rates of 1000, 1450, and 1900 ml/min. Full-scale tests at plant design flow rates were conducted with synthetic sludge in a 48-inch diameter centrifuge also generating 1300 G. Results from both tests are plotted together in Figure 5. The flow rate for the tests with actual sludge have been scaled up using the theoretical relationship: (1)

$$\frac{Q_{small}}{\Sigma_{small}} = \frac{Q_{large}}{\Sigma_{large}}$$

where

Q = feed rate to centrifuge

$\Sigma = \frac{\pi b w^2}{2 g} (3 r_2^2 + r_1^2)$,

area of gravity settling tank with sedimentation performance equivalent to the centrifuge

w = centrifuge rotational velocity, rad/sec

b = centrifuge bowl length

r_2 = centrifuge bowl radius

r_1 = centrifuge weir or pool radius

As shown in Figure 5, the separation behavior of actual and synthetic sludges is quite similar implying a similar correspondence in sludge particle size and density.

Supernate Decontamination

The salts in the spent wash water from sludge washing are concentrated by evaporation and combined with dissolved salt cake to be decontaminated. Cesium will be removed from the clarified solution by ion exchange on "Duolite" ARC-359 resin (trademark of Diamond Shamrock Corporation). Strontium will then be removed from the solution by ion exchange on "Amberlite" IRC-718 resin (trademark of Rohm & Haas). For both cesium and strontium ion exchange, the solution will flow downward through fixed resin beds. When very small amounts of cesium and strontium begin to appear or "break through" in the effluent solution, column operation will be halted. The cesium and strontium sorbed on the beds will be eluted and the beds will be regenerated, thus permitting the cycle to begin again.

Ion exchange processes are conventionally characterized by breakthrough curves in which the concentration of the ion being removed from the solution is plotted as a function of time or column throughput. Figure 6 shows typical cesium breakthrough curves experimentally obtained for both synthetic and actual dissolved salt solutions. Because of the difference in scale of the two tests, the data are plotted in dimensionless form (2). The ordinate shows the ratio of the outlet cesium concentration to the inlet concentration (also referred to as the decontamination factor), while the abcissa is the throughput in column volumes. The inlet concentration of cesium in both cases is about 10^{-4}M while the residence time of the solution in the bed was held constant at 2 column volumes/hour. The test with synthetic supernate was conducted in a plant-height, 8-foot tall column while the actual dissolved salt was decontaminated in 8 cm long laboratory glassware. Because the column residence time was held constant for the two tests, the ratio of fluid linear velocity to column length (V/L) was also constant. Thus, the linear velocity of synthetic supernate through its column was about 30 times faster than that of the actual supernate. Nevertheless, the breakthrough curves for the two tests are very similar. Also shown in Figure 6 is a theoretical breakthrough curve for the columns. Calculations were made using measured resin properties (equilibrium coefficients and particle diffusivities) and the linear equilibrium or J-function model given in reference 1. Both the actual and predicted curves show very steep profiles and a column throughput of 16-17 column volumes at desired breakthrough concentration (DF of 10^4).

The radioisotope content of decontaminated salt cake is being thoroughly characterized to ensure the acceptability of disposing of it as low-level radioactive waste. Table 2 indicates the specific radioactivity present in the salt (about 250 nanocuries/gram) and Figure 7 places this level of radioactivity in perspective with that present in other natural and commercial sources.

Glass Melting

In the reference waste vitrification flowsheet, washed sludge and cesium and strontium eluted from the ion exchange columns are dried in a heated wall spray calciner. For the small-scale hot cell demonstration, the washed sludge was dried instead in a small 5.7 liter fluid-bed calciner, Figure 8. Preheated air is passed upward through the bed at about 280 liters/min for fluidization. The bed is electrically heated to about 350°C by twelve 208-volt cartridge heaters mounted on the outside wall of the dryer. Air discharged from the hot fluidized bed carries with it dry sludge powder and steam from the feed slurry. The dry powder, which is produced at a rate of about 100 g/hr, is separated from the air and steam in a cyclone.

After drying, the waste powder was combined with frit on a 35 wt % waste/65 wt % frit basis and mixed in a V-blender. This mixture was then fed to a small, joule-heated ceramic melter. Figure 9(a) is a plan view, 9(b) is a cross-sectional view and, 9(c) is a photograph of the melter. The main melt chamber is rectangular in shape and about 23 cm long with a pair of Inconel® 690 (trademark of International Nickel) electrodes at the ends of the chamber. The resistance or joule-effect heating generated by passing an electric current through the molten glass provides the necessary energy to maintain the glass at an operating temperature of 1150°C as well as to melt the frit-waste mixture fed to the melter. Normal power requirements of the small-scale melter are about 2-1/2 kW. The molten glass exits the main melt chamber through a small channel or throat at the bottom of the chamber and flows into an overflow or fining chamber. Glass is poured from the fining chamber into 500 ml stainless steel beakers by tilting the melter at a 6-degree angle. Table 3 gives the chemical composition of the borosilicate waste glass.

The melting behavior and rate for both synthetic and actual waste in the small-scale melter were comparable. Maximum melting rates were about 8 grams of dried feed per minute. The melting rate is governed by the rate at which heat can be generated within the molten glass and convected to the surface to melt freshly added feed. A major limitation on melting rate of SRP waste can be the formation of a persistent long-lived foam. Foam can blanket the melt surface and significantly reduce the rate at which feed material can fall to the melt surface and heat can be transferred to the particles of feed. In severe cases, the foam can even flood the melt chamber. Analysis of the bubbles of foam from SRP waste vitrification revealed that the gas in the bubbles was primarily oxygen, probably released when the iron and perhaps manganese oxides in the waste are reduced to lower valence states in the melt. Conventional glass industry practice in such cases (3) is to add a small amount of reducing agent, such as carbon, to the feed. This promotes reduction of the oxides and release of gas in the dry feed material at the top of the melt where it can readily escape rather than form a foam.

Addition of approximately stoichiometric quantities of carbon to the feed was found to be highly effective in minimizing foam formation with both actual and synthetic SRP waste.

The design of the glass melter for the reference DWPF process, Figure 10, is significantly different from that of the small-scale melter. Because of the differences in geometry, convective mixing, and heat transfer, the throughput performance of the small melter cannot be simply scaled to give potential plant performance data as was previously done for the sludge washing and supernate decontamination operations.

Off-Gas Characteristics

Some of the components of the waste are at least partially volatile at the 1150°C operating temperature of the melter. Elements that will volatilize and are of special concern include Ru, I, Cs, Hg, Cl, and F. After volatilizing from the melt, the vapors of these elements will pass through cooler sections of the melter and calciner, Figure 10, before reaching the off-gas scrubbing system. As they pass through these cooler sections, they may condense or react and plate out on melter and calciner surfaces and contribute to corrosion or plugging concerns.

To begin characterizing the behavior of semivolatile components generated during vitrification of actual SRP waste, a semivolatile trap was installed on the small-scale melter. The semivolatile trap, Figure 11, was a stainless steel 9/16-inch diameter tube containing a stack of concentric 1/2-inch diameter rings. The entrance of the trap was placed about one inch from the melt surface. Thermocouples were installed at each end of the ring stack and each ring was assigned a temperature based on an assumed linear gradient between the measured inlet temperature of $800^{\circ}C$ and the exit temperature of $130^{\circ}C$. Off-gas from the melter passed through the stacked rings and into an off-gas scrubbing system. The inside walls of the rings provided a surface for deposition of condensing volatiles or reaction products. After an experiment, the rings were individually leached with aqueous solutions to quantify deposition on each ring.

Figures 12 and 13 show the measured deposition pattern for two of the elements of concern, Cs and Ru. As shown in Figure 13, the Cs deposited in a regular pattern with about 70% of that vaporized from the melt surface depositing on rings at temperatures greater than $350^{\circ}C$, the temperature of the sintered metal filters in the DWPF calciner/melter. In contrast to this, Figure 14 indicates no regular pattern for the ruthenium deposition in four different experiments. Rather, it seemed to collect randomly on the rings. The elusive performance of ruthenium will come as no surprise to those who have worked with it. Ruthenium is generally believed to be volatilized, as RuO_4, in high temperature applications but can rapidly undergo thermal decomposition to form finely divided particulates of RuO_2 (4). This behavior would be consistent with the deposition patterns observed in this work; the ruthenium decomposed to the solid dioxide homogeneously and stuck wherever it encountered a hospitable surface. In the DWPF application, much of the ruthenium would remain in the calciner/melter but some of it will pass through the filters to be removed from the off-gas by water scrubbing and sorption on a silica gel bed.

CONCLUSIONS

Experiments have been made to demonstrate the feasibility of immobilizing SRP high-level waste in borosilicate glass. Results to date are encouraging. Equipment performance and processing characteristics for solidifying small batches of actual SRP waste have agreed reasonably well with previous small and large scale experience with synthetic waste, and with theoretical predictions.

TABLE I

Chemical Composition of SRP Sludge and Supernate

Soluble Salts in Supernate[a]	Wt %	Insoluble Solids in Sludge	Wt %
$NaNO_3$	46.9	$Fe(OH)_3$	38.5
$NaNO_2$	18	$UO_2(OH)_2$	2.91
$NaAlO_2$	9.71	$CaCO_3$	3.82
$NaOH$	7.24	$Ni(OH)_2$	4.42
Na_2CO_3	7.54	Na_2O	1.91
Na_2SO_4	10.1	$NaNO_3$	1.13
$Na_2C_2O_4$	0.123	Na_2SO_4	0.609
$NaCl$	0.305	MnO_2	7.58
NaF	0.199	$Hg(OH)_2$	1.16
$Na[HgO(OH)]$	0.0608	$NaCl$	1.22
		NaF	0.128
		C	1.30
		$Al(OH)_3$	34.4
		SiO_2	0.557
		HgI_2	0.376

---

[a] Supernate feed is constituted to $\sim$29 wt % salt solution by dissolving the salt cake in the tank with recycle water.

TABLE II

Specific Radioactivity of Decontaminated Saltcake

Radionuclide	Concentration (nCi/gr)	DF
Cs^{137}	31	1.7 x 10^{4}
Ba^{137m}	31	-
Cs^{134}	0.28	1.7 x 10^{4}
Sr^{90}	0.4	900
Y^{90}	0.4	-
Ru^{106}	28	
Rh^{106}	28	
Sb^{125}	3.5	
Sb^{126m}	0.24	
Sn^{126}	0.24	
Pu^{238}	1.9	30
Co^{60}	<0.0015	
Ag^{110m}	<0.0085	
Ce^{144}-Pr^{144}	<1.10	
Eu^{152}	<0.0075	
Eu^{154}	<0.021	
Zr^{95}-Nb^{95}	<0.013	
H^{3}	100 total	
Tc^{99}		
I^{129}		
Pm^{147}		
Sm^{151}		
Sn^{121n}		

TABLE III

Chemical Composition of Borosilicate Glass Waste Form

Oxide	Source	Amount, wt %
Li_2O	F	2.84
B_2O_3	F	7.11
TiO_2	F	7.11
CaO	F + S	4.49
Na_2O	F + S	16.12
SiO_2	F + S	38.41
Fe_2O_3	S	12.65
Al_2O_3	S	2.57
MnO_2	S	3.33
U_3O_8	S	1.18
NiO	S	1.56
Zeolite		2.63
Density		2.37 g/cc @ 1150°C 2.8 g/cc @ 120°C

---

*F = Frit; S = composite sludge

REFERENCES

1. J. H. Perry, Ed., Chemical Engineers' Handbook, 4th Edition, McGraw-Hill Book Company, New York (1968).

2. Friedrich Helfferich, Ion Exchange, McGraw-Hill Book Company, New York (1962).

3. W. H. Manning and R. E. Davis, "Controlling Redox Conditions in Glass Melting", Glass Industry, Vol. 59 No. 5, p. 13 (May 1978).

4. S. J. Rimshaw, F. N. Case, and J. A. Tompkins, "Volatility of Ruthenium-106, Technetium-99, and Iodine-129, and the Evolution of Nitrogen Oxide Compounds During the Calcination of High-Level, Radioactive Nitric Acid Waste", Oak Ridge National Laboratory Report ORNL-SS62, (1980).

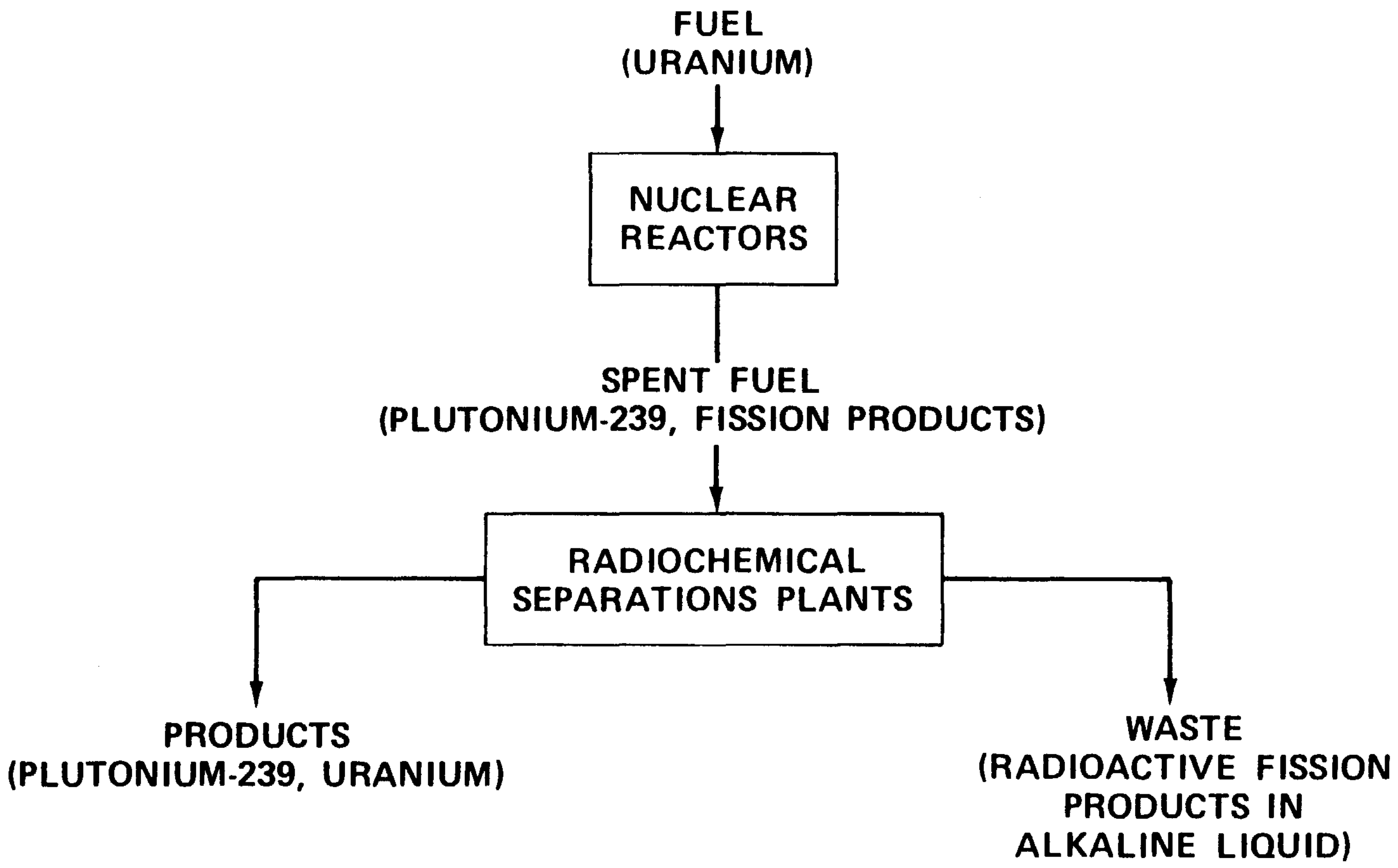

Figure 1. Source of Radioactive Wastes at Savannah River

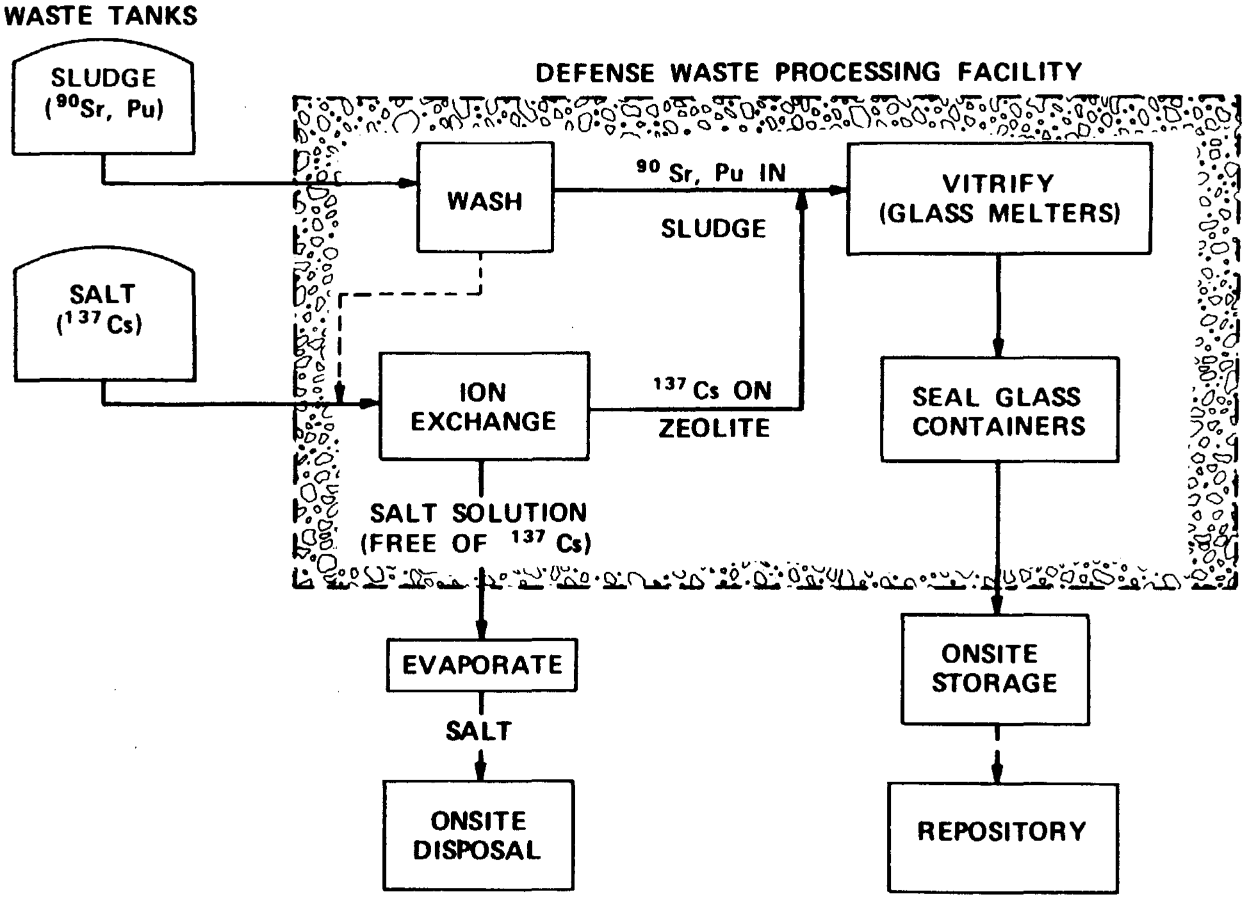

Figure 2. Reference Process for SRP Waste

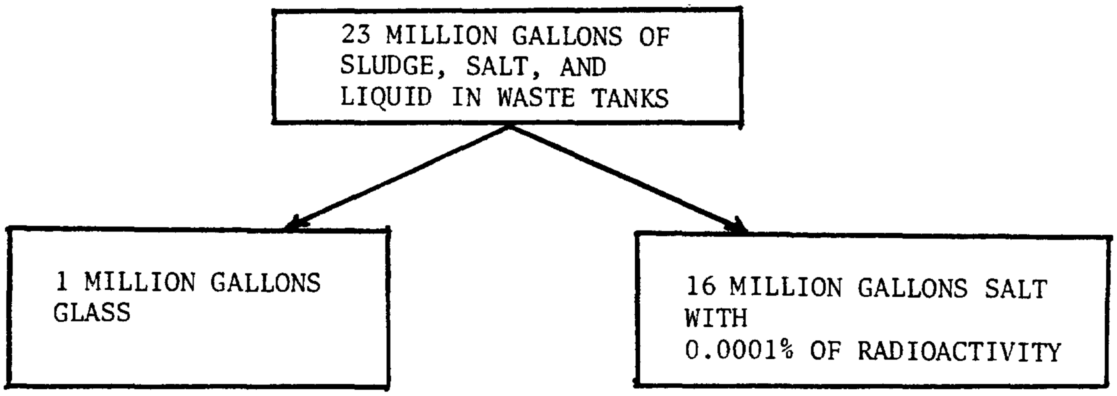

Figure 3. Disposition of Waste Inventory

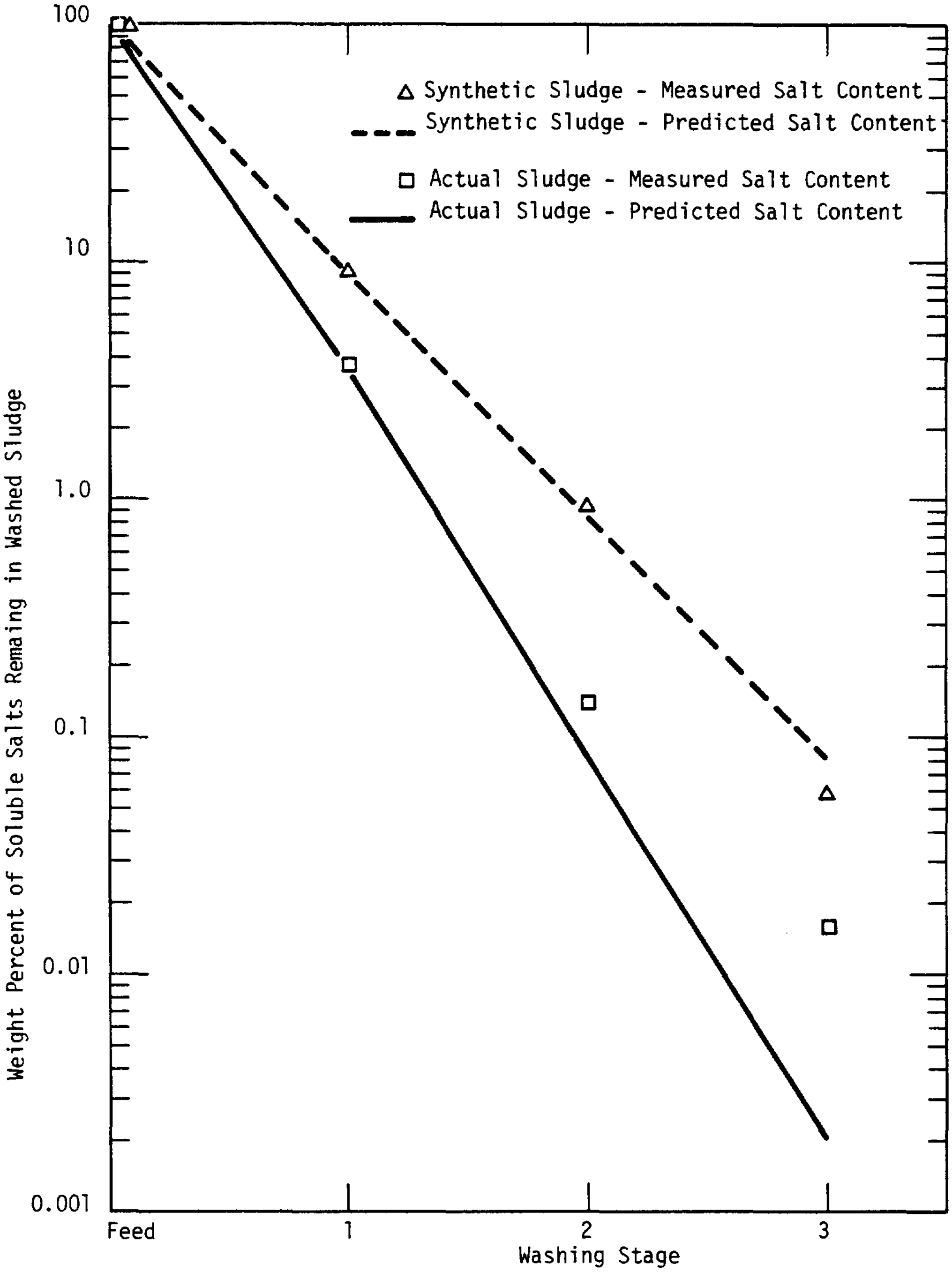

Figure 4. Sludge Washing by Dilution Model

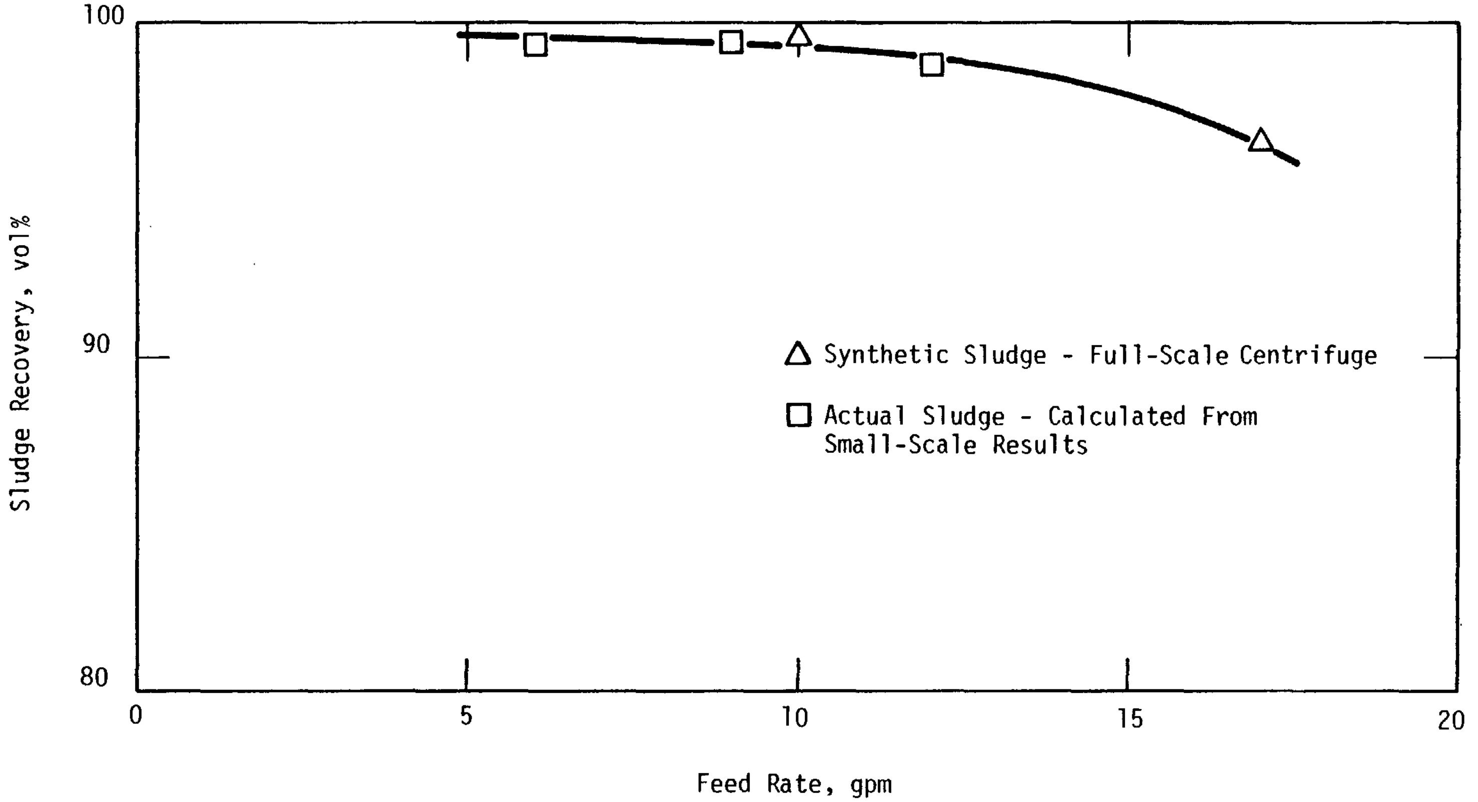

Figure 5. Sludge Recovery in Centrifuge

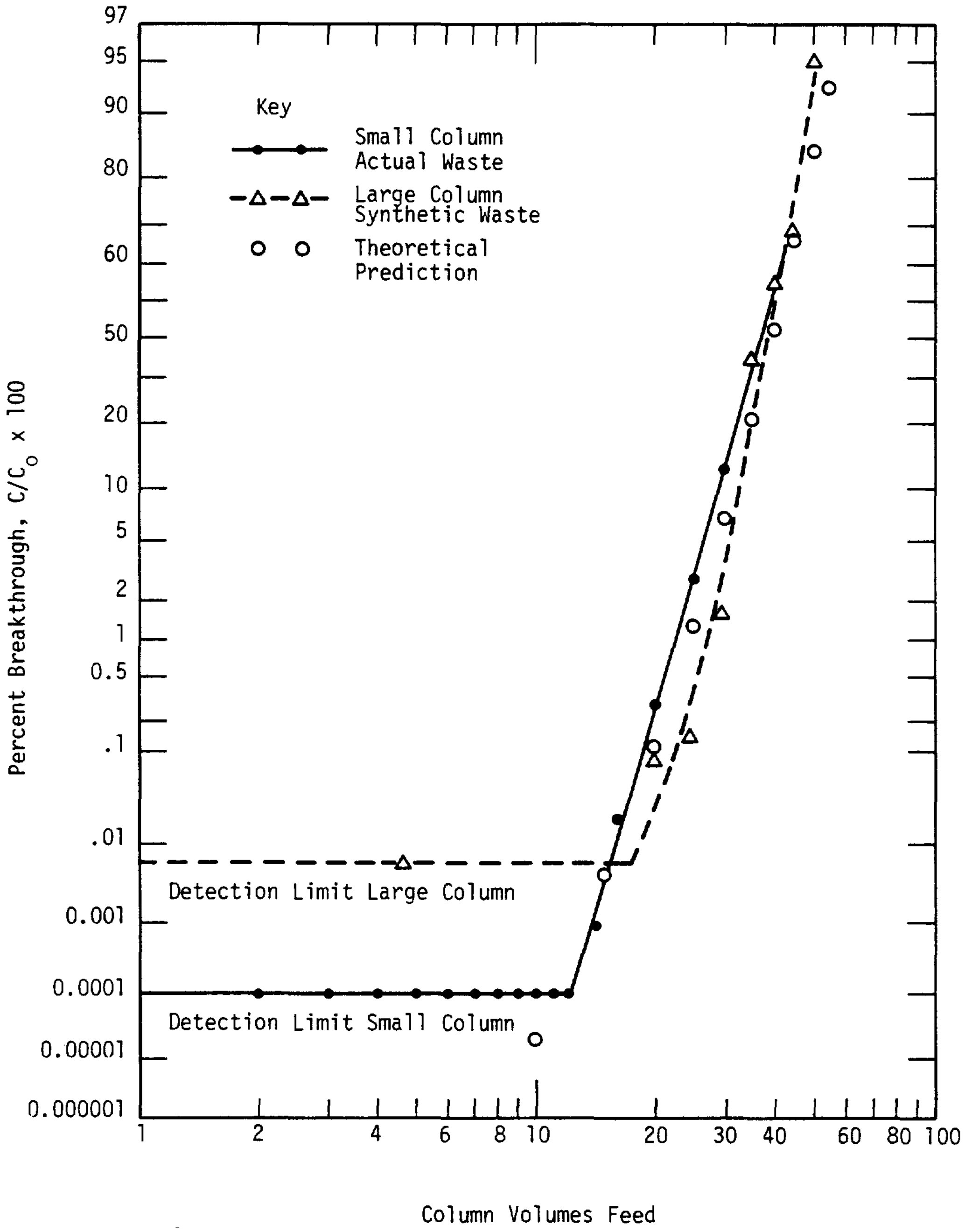

Figure 6. Performance of Cesium Ion Exchange Columns

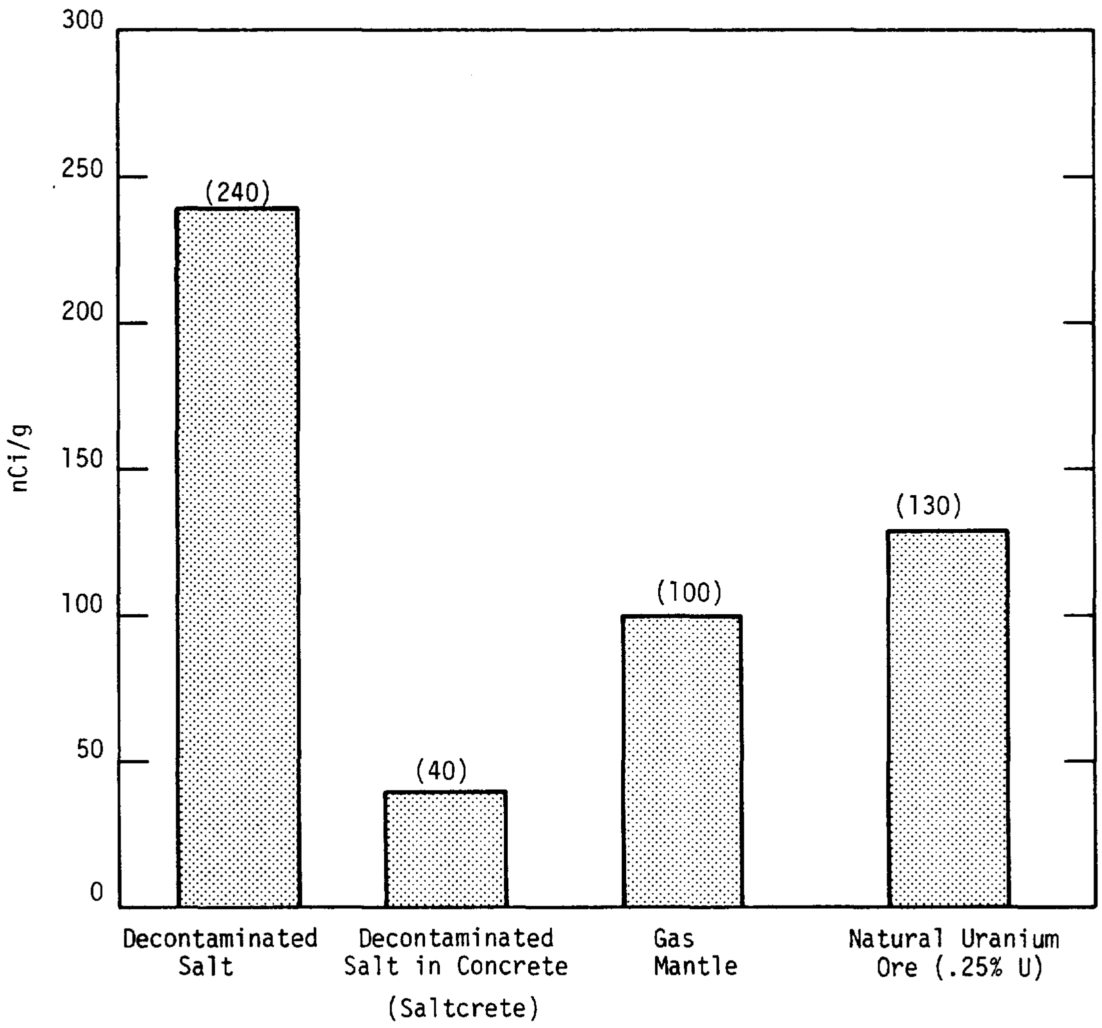

Figure 7. Residual Radioactivity of Decontaminated Salt

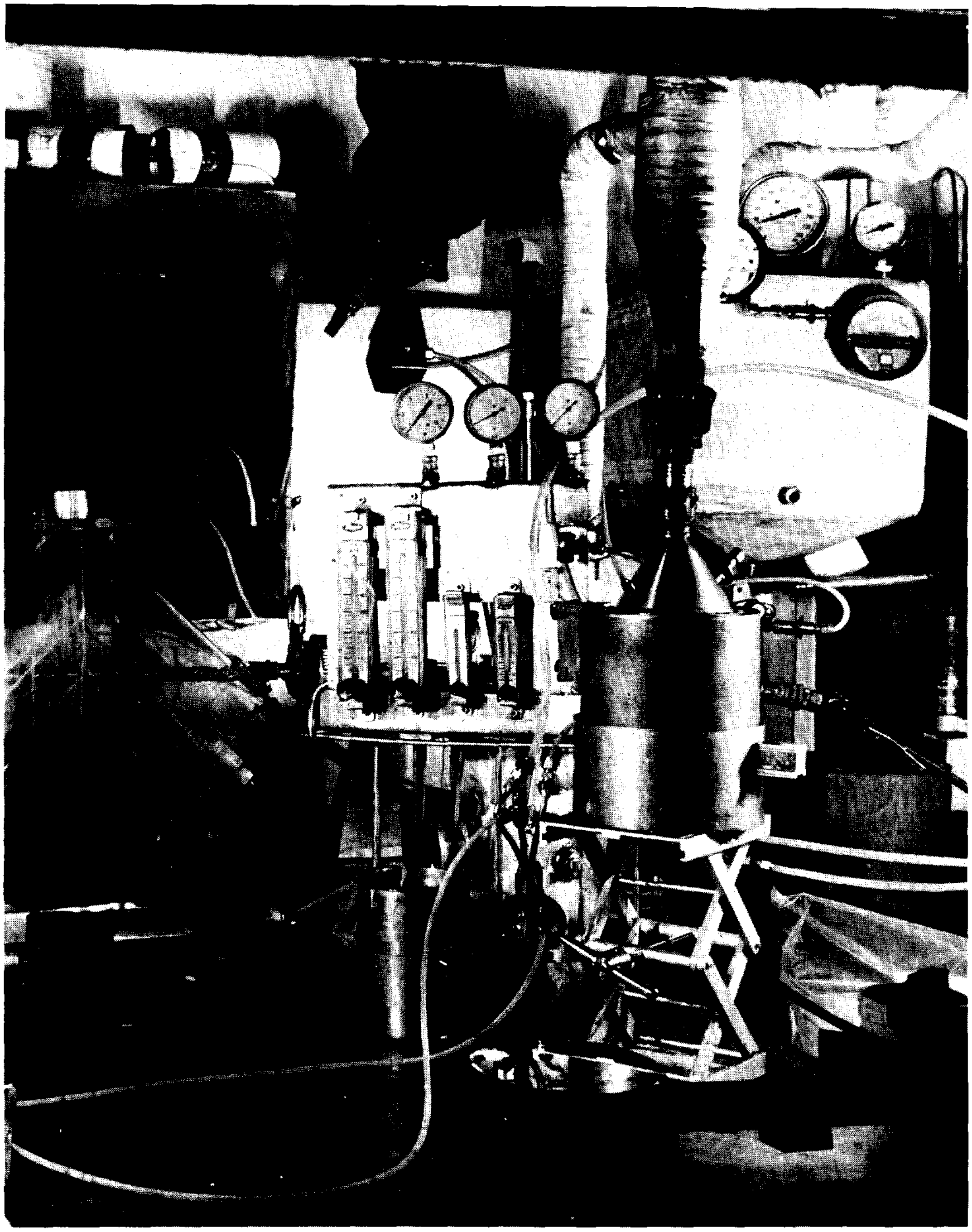

Figure 8. Fluid Bed Calciner and Calcine-Frit V-Blender

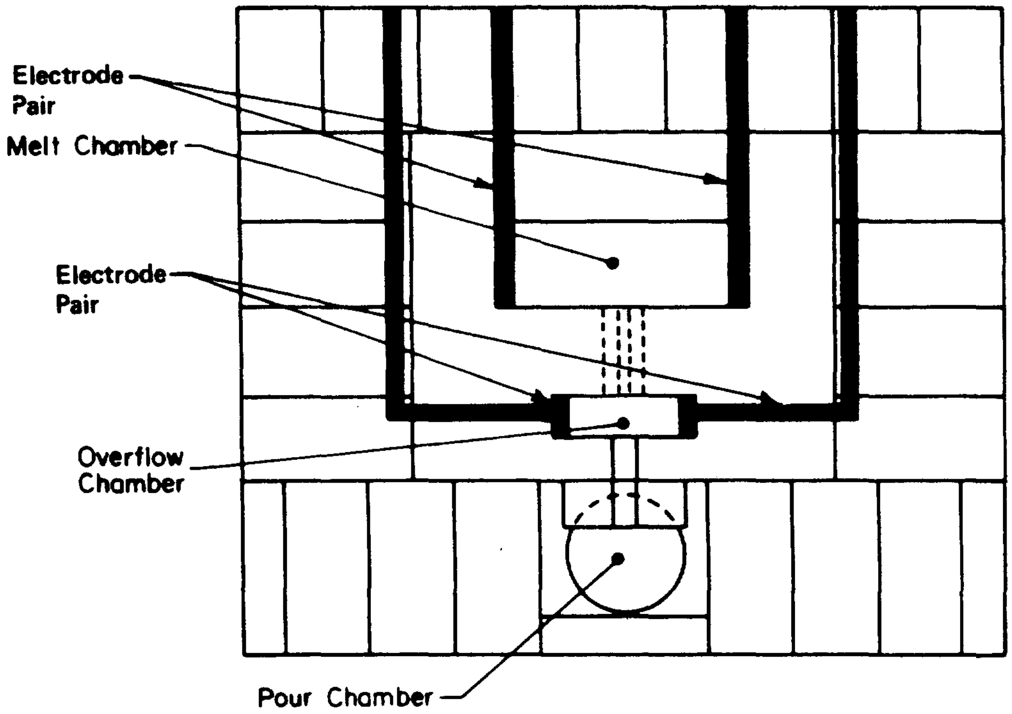

(a) Plan View

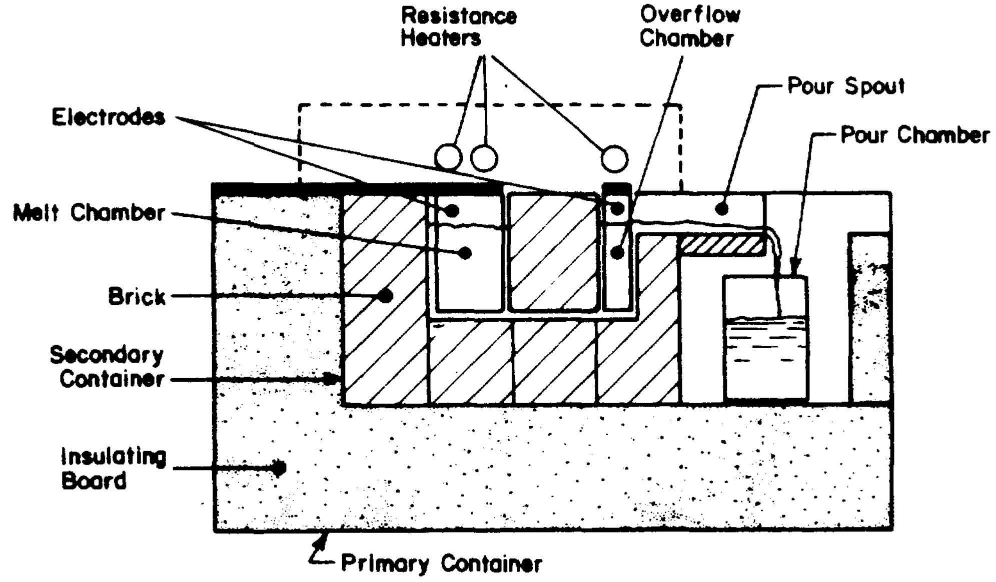

(b) Cross-Section View

Figure 9. Small Scale Melter

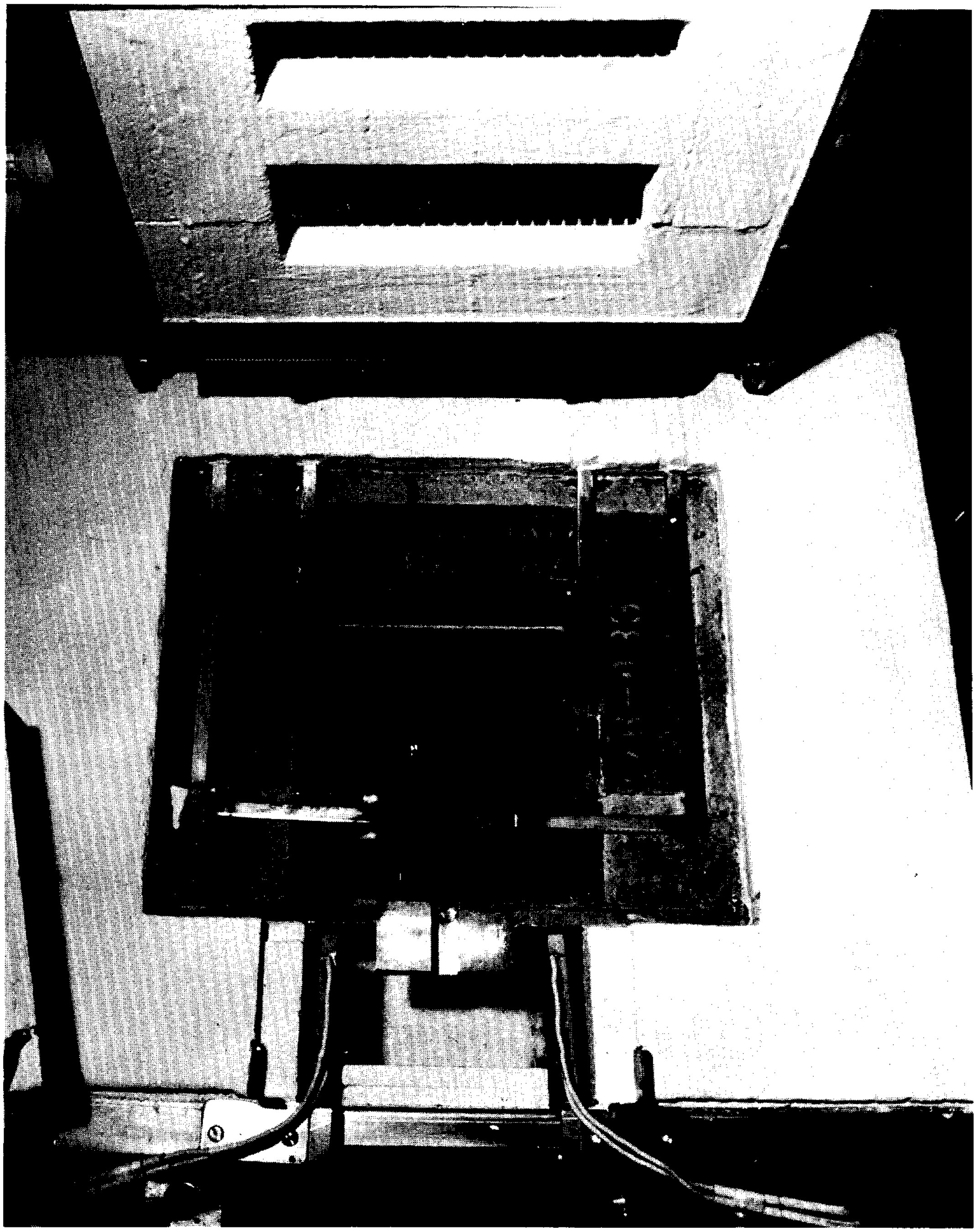

Figure 9(c). Small Scale Melter

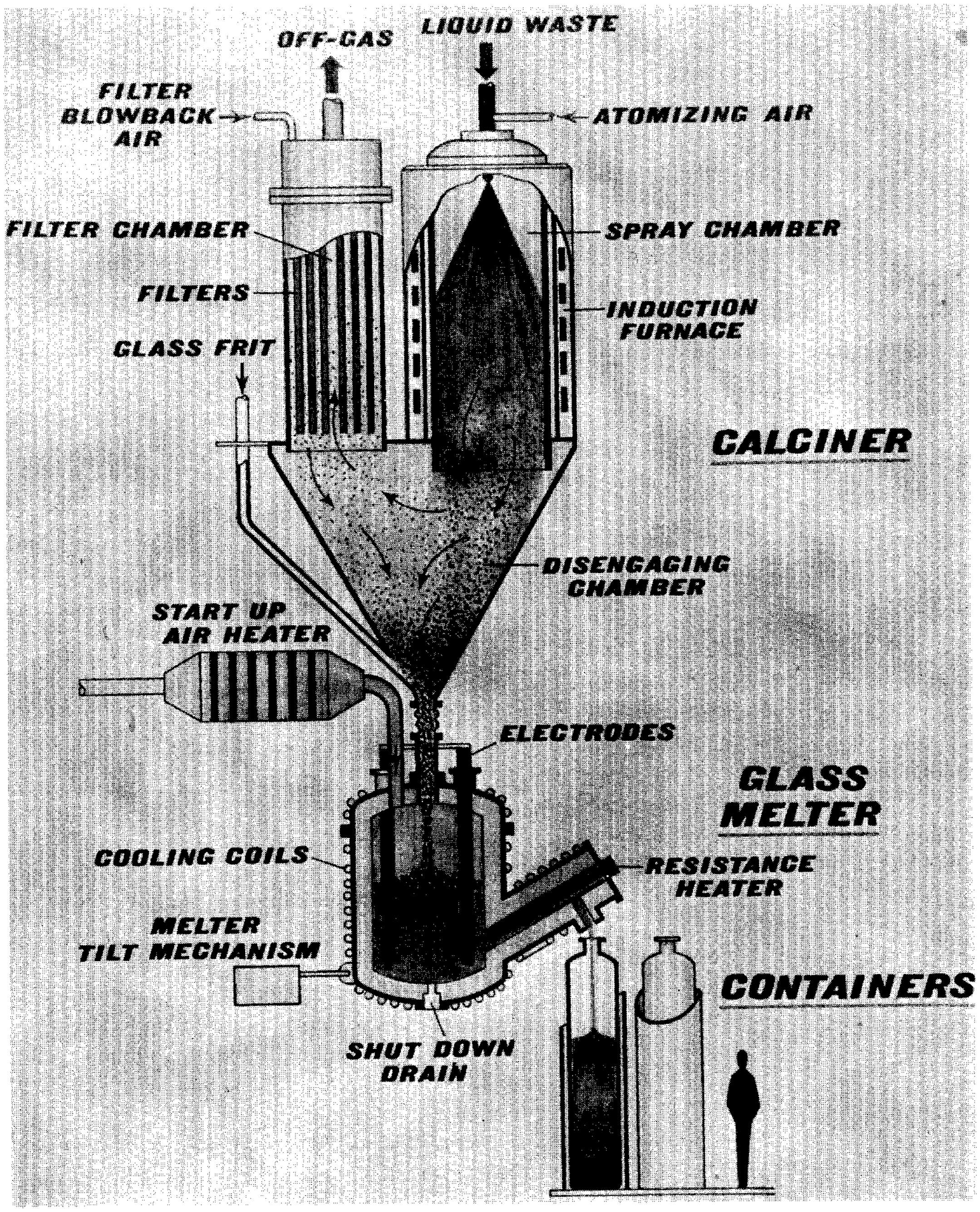

Figure 10. Schematic of Full-Scale Calciner-Melter

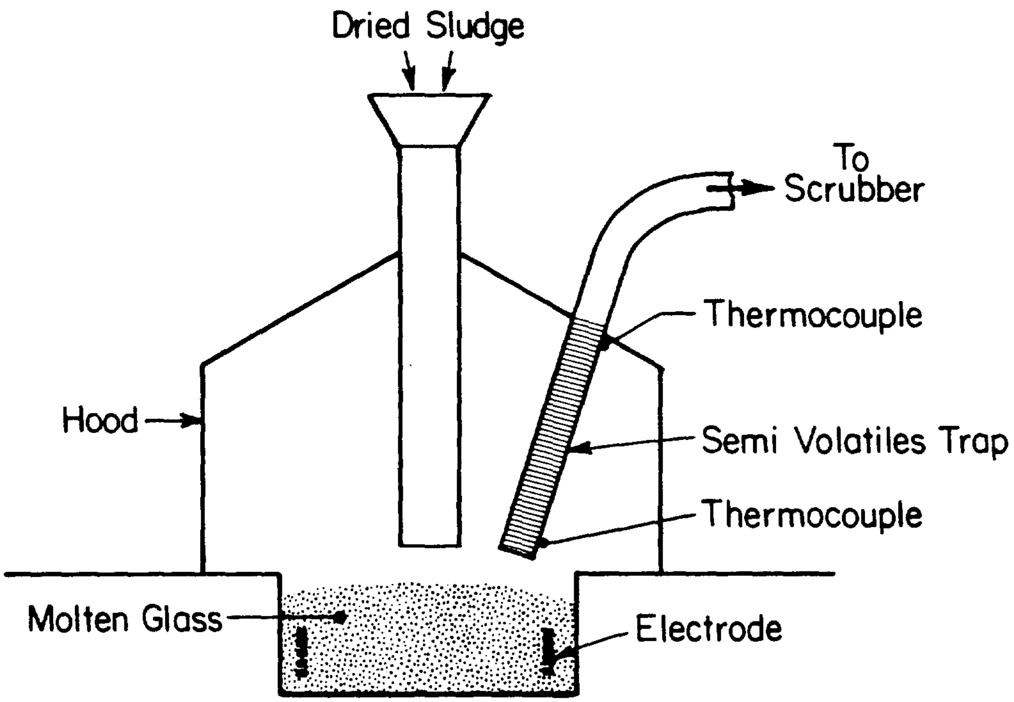

Figure 11. Schematic of Lab-Scale Melter

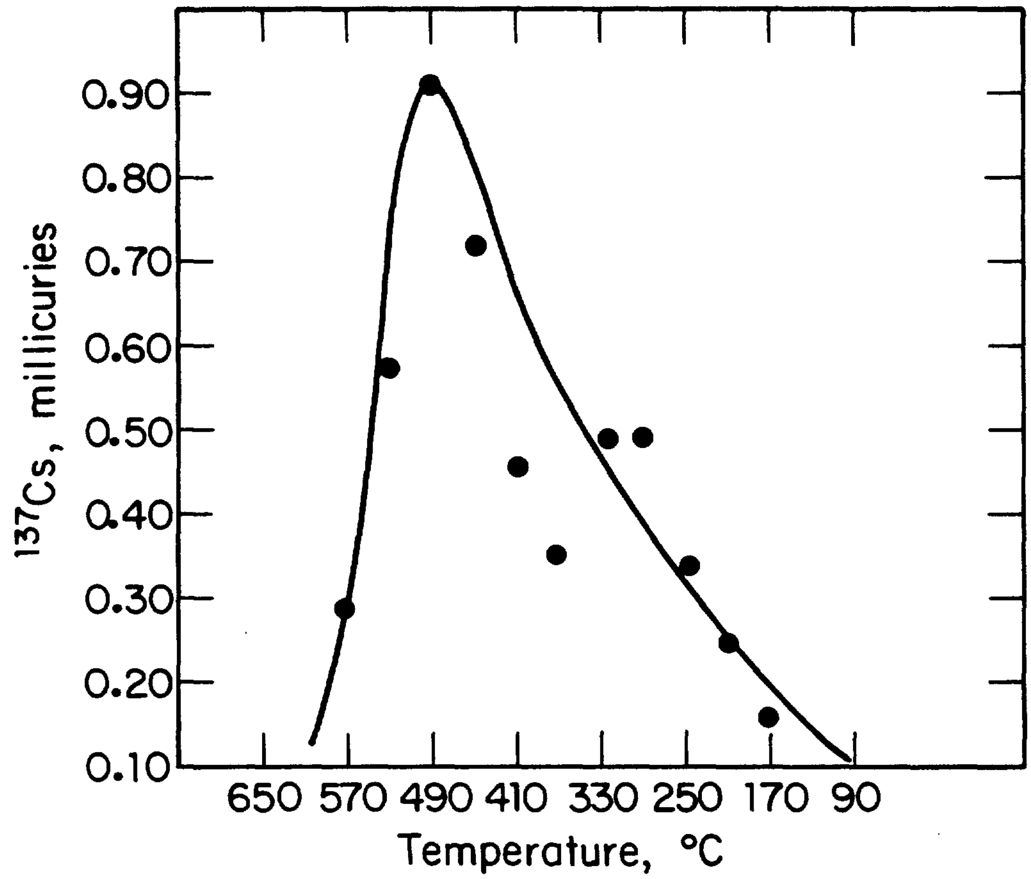

Figure 12. Deposition of ^{137}Cs in the Semivolatiles Trap

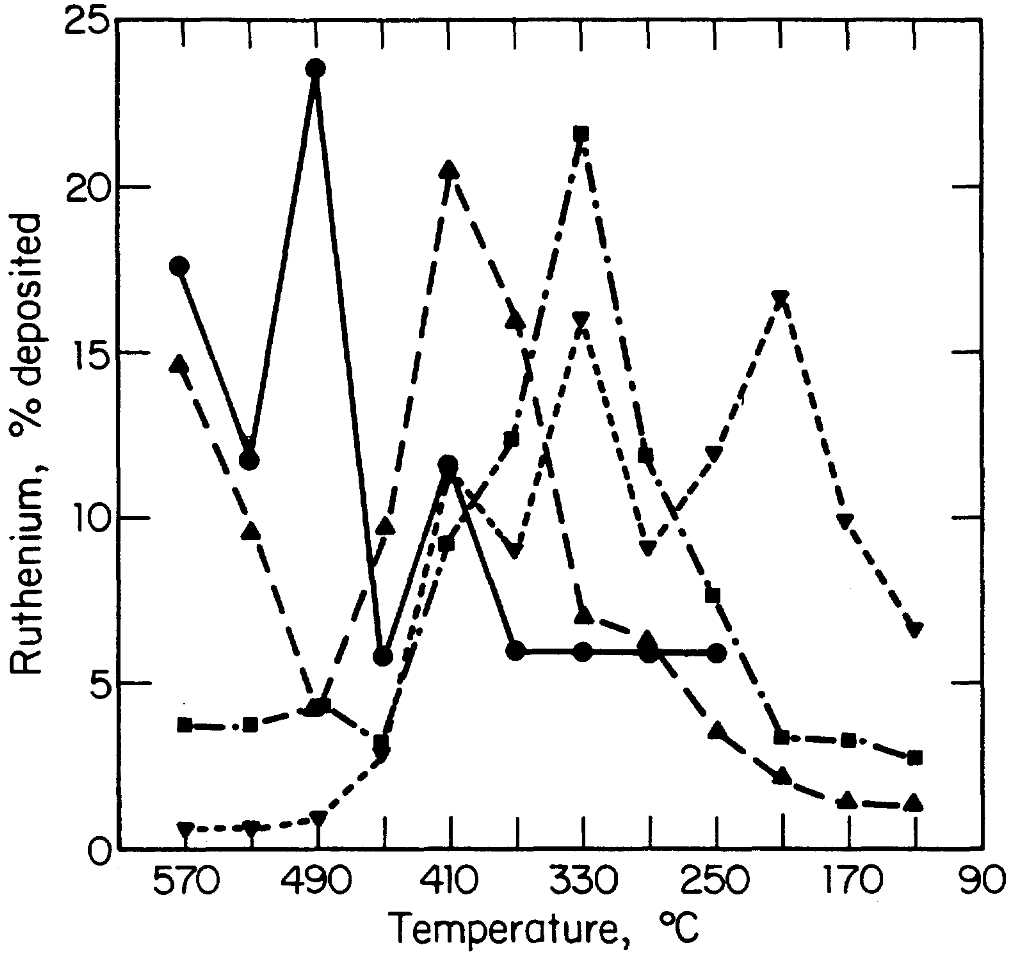

Figure 13. Deposition of Ru in the Semivolatiles Trap